A Generalized Multiple-Input, Multiple-Output Modal Parameter Estimation Algorithm

Roy R. Craig Jr.* and Mark A. Blair†
The University of Texas at Austin, Austin, Texas

A new method for experimental determination of the modal parameters of a structure is presented. The method allows for multiple-input forces to be applied simultaneously and for an arbitrary number of acceleration response measurements to be employed. These data are used to form the equations of motion for a damped linear elastic structure. The modal parameters are then obtained through an eigenvalue technique. In conjunction with the development of the equations, an extensive computer simulation study was performed. The results of the study show a marked improvement in the mode shape identification for closely-spaced modes as the number of applied forces is increased. Also demonstrated is the influence of noise on the method's ability to identify accurate modal parameters. Here again, an increase in the number of exciters leads to a significant improvement in the identified parameters.

Nomenclature

$[/A/]$	= diagonal modal admittance matrix, $(m \times m)$, $= -w^2/[(w_r^2 - w^2) + i(2\xi_r w w_r)]$, $r = 1,m$
$[C_i]$	= damping matrix defined by Eq. (7)
$[D]$	= force distribution matrix defined by Eq. (2)
$\{F(w)\}$	= Fourier-transformed input force vector, $(n \times 1)$
$[H(w)]$	= complex frequency response function matrix, $(n \times n)$, $= [\phi][/A/][\phi]^T$
$[K_i]$	= stiffness matrix defined by Eq. (7)
$[M_i]$	= mass matrix defined by Eq. (7)
m	= number of modes active in a given frequency range, or modal degrees of freedom
n	= number of acceleration measurement stations, or physical degrees of freedom
$[T],[Y],[Z]$	= matrices defined by Eqs. (11) and (12)
w	= circular frequency
w_r	= circular natural frequency of mode r
$\{\ddot{X}_i(w)\}$	= acceleration at independent stations, $(m \times 1)$
$\{\ddot{X}_d(w)\}$	= acceleration at dependent stations, $(n-m) \times 1)$
λ	= eigenvalue defined by Eq. (17)
ξ_r	= damping ratio of mode r
$[\phi]$	= modal matrix, $(n \times m)$

Introduction

THE need for modal testing (sometimes referred to as modal analysis) of structures is well known and documented. The problem is that there is no fool-proof and highly efficient method to extract modal coefficients from structural test data. Over the past 40 years several different types of analysis have been developed and practiced with varying degrees of success. These analyses range from the time-honored multi-shaker sine dwell test[1] and its recent variations[2] to the newer time-domain analyses: the least-squares curve-fitting time-domain method[3] and the Ibrahim time-domain method.[4,5] For several years, since the advent of digital computers and the development of the fast Fourier transform (FFT), considerable time has gone into developing frequency domain analyses. Several methods have been developed which produce frequency response functions (FRFs) of a structure, using either single-point excitation[6] or multipoint excitation.[7] There are also many algorithms which estimate the modal parameters from the FRFs.[8-14]

Although the principal results sought in a modal analysis are the modal parameters, i.e., undamped or damped natural frequencies, damping factors, and mode shapes, several authors have addressed the problem of determining the system matrices $[M]$, $[C]$, and $[K]$.[15,16] Leuridan et al.[15] developed an algorithm that identifies system matrices of order equal to the number of generalized coordinates used to describe the system. Constraints such as bandedness and symmetry may be invoked to reduce the total number of system parameters to be identified. Reference 16 also describes a method for computing $[M]$, $[C]$, and $[K]$, but a serious disadvantage of this method is that it requires measurement of displacements and velocities as well as accelerations.

Development of a New Multi-Shaker Algorithm

A technique to avoid problems associated with single-point testing is to apply forces at multiple locations.[14] The method to be developed in this paper is an extension of the simultaneous frequency domain (SFD) method described by Coppolino.[13]

The attractive features of the present method are:

1) Simultaneous multipoint excitation, with several possible forms of input time history, is permitted.

2) Reduced $[M]$, $[C]$, and $[K]$ matrices are estimated, and these are used to compute a consistent set of modal parameters for a selected frequency range.

3) Fourier transforms of acceleration responses and force inputs are employed.

4) Mode shapes are computed which include all generalized response coordinates.

5) The algorithm is conceptually straightforward.

6) The method is stable in the presence of random noise.

Development of Basic Algorithm

The multi-shaker modal analysis (MSMA) method presented herein assumes that a linear structure can be described accurately over a limited frequency range by a finite number of modal degrees of freedom (DOFs). This assumption yields the standard frequency domain matrix equation relating the

Received March 8, 1984; presented as Paper 84-1050 at the AIAA Dynamics Specialists Conference, Palm Springs, Calif., May 17-18, 1984; revision received Aug. 5, 1984.

*Professor, Aerospace Engineering and Engineering Mechanics. Associate Fellow AIAA.

†Graduate Student, Aerospace Engineering; presently with Lockheed Missiles and Space Corporation, Sunnyvale, Calif.

output accelerations at given points on the structure to the input forces

$$\{\ddot{X}(w)\} = [H(w)]\{F(w)\} \tag{1}$$

The force vector is rewritten in a form that includes only the physical DOFs where forces are applied. A distribution matrix relates this new force vector, $\{f(w)\}$, to the original force vector, $\{F(w)\}$.

$$\{F(w)\} = [D]\{f(w)\} \tag{2}$$

For example, if a four-DOF system has exciters at points 1 and 3, the equation would be

$$\{F(w)\} = \begin{Bmatrix} f_1 \\ 0 \\ f_3 \\ 0 \end{Bmatrix} = \begin{bmatrix} 1 & 0 \\ 0 & 0 \\ 0 & 1 \\ 0 & 0 \end{bmatrix} \begin{Bmatrix} f_1 \\ f_3 \end{Bmatrix}$$

Therefore, Eq. (1) is now

$$\{\ddot{X}(w)\} = [\phi]\,[/A/]\,[\phi]^T[D]\{f(w)\} \tag{3}$$

The form of $[/A/]$ given in the Nomenclature implies that the algorithm presented in this paper applies only to systems having "proportional" damping. However, this restriction can be relaxed without difficulty. It is assumed that there are n physical DOFs where the responses are measured. If it is also assumed that the structure can be described accurately over the frequency range of interest by m DOFs ($m<n$), then Eq. (3) can be partitioned into sets of independent and dependent equations. Thus,

$$\begin{Bmatrix} \ddot{X}_i(w) \\ \ddot{X}_d(w) \end{Bmatrix} = \begin{bmatrix} [\phi_i] \\ [\phi_d] \end{bmatrix} [/A(w)/] \left[[\phi_i]^T [\phi_d]^T \right] \begin{bmatrix} [D_i] \\ [D_d] \end{bmatrix} \{f(w)\} \tag{4}$$

or

$$\begin{Bmatrix} \ddot{X}_i(w) \\ \ddot{X}_d(w) \end{Bmatrix} = \begin{bmatrix} [I] \\ [\phi_d][\phi_i]^{-1} \end{bmatrix} [\phi_i]\,[/A(w)/]\,[\phi_i]^T[D_{id}]\{f(w)\} \tag{5}$$

where

$$[D_{id}] = [D_i] + [\phi_i]^{-T}[\phi_D]^T[D_d]$$

From Eq. (5) a relationship between the independent and dependent accelerations is

$$\{\ddot{X}_d(w)\} = [\phi_d][\phi_i]^{-1}\{\ddot{X}_i(w)\} \tag{6a}$$

This equation will be employed later to determine the modal vector elements of the dependent DOFs for the identified natural frequencies. The equation relating the independent accelerations to the forces is

$$\{\ddot{X}_i\} = [\phi_i]\,[/A(w)/]\,[\phi_i]^T[D_{id}]\{f(w)\} \tag{6b}$$

Premultiplying both sides of Eq. (6b) by

$$\left[[\phi_i]\,[/A(w)/]\,[\phi_i]^T \right]^{-1}$$

and expanding yields

$$\left[[\phi_i]\,[/A(w)/]\,[\phi_i]^T \right]^{-1}\{\ddot{X}_i\} = [D_{id}]\{f(w)\}$$

$$[\phi_i]^{-T}[/(1/A(w))/]\,[\phi_i]^{-1}\{\ddot{X}_i\} = [D_{id}]\{f(w)\}$$

$$[\phi_i]^{-T}[/(1-i2\xi_r(w_r/w)-(w_r/w)^2)/]\,[\phi_i]^{-1}\{\ddot{X}_i\} = [D_{id}]\{f(w)\}$$

$$[\phi_i]^{-T}[\phi_i]^{-1}\{\ddot{X}_i\} + [\phi_i]^{-T}[/2\xi_r w_r/]\,[\phi_i]^{-1}(-i/w)\{\ddot{X}_i\} + [\phi_i]^{-T}[/w_r^2/]\,[\phi_i]^{-1}(-1/w^2)\{\ddot{X}_i\} = [D_{id}]\{f(w)\}$$

or, in summary,

$$[M_i]\{\ddot{X}_i\} + [C_i]\{\dot{X}_i\} + [K_i]\{X_i\} = [D_{id}]\{f(w)\} \tag{7}$$

where

$$[M_i] = [\phi_i]^{-T}[\phi_i]^{-1}$$

$$[C_i] = [\phi_i]^{-T}[/2\xi_r w_r/]\,[\phi_i]^{-1}$$

$$[K_i] = [\phi_i]^{-T}[/w_r^2/]\,[\phi_i]^{-1}$$

$$\{\dot{X}_i\} = (-i/w)\{\ddot{X}_i\}$$

$$\{X_i\} = (-1/w^2)\{\ddot{X}_i\}$$

Least-squares averaging may be employed to estimate the matrices $[M_i]$, $[C_i]$, and $[K_i]$. Therefore, the accelerations, velocities, displacements, and forces in Eq. (7) are expanded into matrices, where each column corresponds to a discrete frequency. That is,

$$[\ddot{X}_i] = [\ddot{X}_i(w_1)\,|\ddot{X}_i(w_2)|\ldots|\ddot{X}_i(w_k)] \tag{8}$$

where $k>m$. Multiplication of Eq. (7) by $[M_i]^{-1}$ yields

$$-[\ddot{X}_i] = \left[[\tilde{C}_i]\,[\tilde{K}_i]\,[\tilde{D}_{id}] \right] \begin{bmatrix} [\dot{X}_i] \\ [X_i] \\ [f(w)] \end{bmatrix} \tag{9}$$

where

$$[\tilde{C}_i] = [M_i]^{-1}[C_i] \tag{10a}$$

$$[\tilde{K}_i] = [M_i]^{-1}[K_i] \tag{10b}$$

$$[\tilde{D}_{id}] = -[M_i]^{-1}[D_{id}] \tag{10c}$$

Since $[\tilde{C}_i]$, $[\tilde{K}_i]$, and $[\tilde{D}_{id}]$ are real matrices, Eq. (9) can be rewritten for the real and imaginary parts of the responses and inputs.

$$-\left[[\ddot{X}_{i_{\mathrm{Re}}}]\,[\ddot{X}_{i_{\mathrm{Im}}}] \right] = \left[[\tilde{C}_i]\,[\tilde{K}_i]\,[\tilde{D}_{id}] \right] \begin{bmatrix} [\dot{X}_{i_{\mathrm{Re}}}] & [\dot{X}_{i_{\mathrm{Im}}}] \\ [X_{i_{\mathrm{Re}}}] & [X_{i_{\mathrm{Im}}}] \\ [f_{\mathrm{Re}}] & [f_{\mathrm{Im}}] \end{bmatrix} \tag{11}$$

Since this equation is overdetermined ($k>m$), a least-squares solution is used. Equation (11) may be rewritten symbolically as

$$[Y] = [T]\,[Z] \tag{12}$$

The least-squares solution for $[T]$ is

$$[T] = [Y][Z]^T\left[[Z][Z]^T\right]^{-1} \tag{13}$$

The $[\tilde{C}_i]$ and $[\tilde{K}_i]$ that were solved for in Eq. (13) now can be used to determine the eigenvalues and eigenvectors for the system in the following manner. From Eq. (9) the free-vibration equation

$$\ddot{X}_i + [\tilde{C}_i]\dot{X}_i + [\tilde{K}_i]X_i = 0 \tag{14}$$

may be written. Since the matrices $[\tilde{C}_i]$ and $[\tilde{K}_i]$ are constant, X_i and its derivatives in Eq. (14) may be written in the time domain, rather than in the frequency domain as originally expressed in Eq. (7). Thus, let

$$X_i = \chi e^{\lambda t} \tag{15a}$$

$$\dot{X}_i = \lambda X_i \tag{15b}$$

$$\ddot{X}_i = \lambda \dot{X}_i \tag{15c}$$

From Eq. (15b)

$$\lambda X_i - \dot{X}_i = 0 \tag{16}$$

Thus, combining Eqs. (14) and (15) yields

$$\lambda\begin{Bmatrix}\dot{X}_i\\ X_i\end{Bmatrix} + \begin{bmatrix}[\tilde{C}_i] & [\tilde{K}_i]\\ [-I] & [0]\end{bmatrix}\begin{Bmatrix}\dot{X}_i\\ X_i\end{Bmatrix} = \begin{Bmatrix}0\\ 0\end{Bmatrix} \tag{17}$$

which is a standard linear eigenvalue problem. The eigenvectors will produce mode shape components for the independent DOFs only. To include the dependent DOFs, Eq. (6a) is expanded to matrix form for the k frequency points and then manipulated, via the least-squares technique, to produce a relationship between the dependent and independent elements of the modal vectors.

$$[\ddot{X}_d] = [\phi_d][\phi_i]^{-1}[\ddot{X}_i]$$

$$[\phi_d] = [\ddot{X}_d][\ddot{X}_i]^T\left[[\ddot{X}_i][\ddot{X}_i]^T\right]^{-1}[\phi_i] \tag{18}$$

Forcing Functions

As indicated by Eqs. (4) and (5), the forces may be applied at the dependent as well as independent DOFs. This feature of the equations allows the forces to be applied either where accelerations could not be measured or where an accelerometer produced bad readings and was subsequently discarded. It also allows the user more freedom in determining which locations are to be identified as independent DOFs. If, after data acquisition is completed and a general analysis done, it is determined that a particular DOF is not important; its responses can be reduced out of further calculations, even though it was forced.

In addition to the freedom of location of forces, there is also a freedom in the type of forces that can be applied, subject to one constraint. From Eq. (13) it is seen that, if two forces are fully coherent, the inverse of the matrix will be singular. However, the restriction is not too severe. If two forcing functions are identical, only one forcing function needs to be included in the force array. The force distribution matrix will handle the duplication in the applied force spectra. Since, in reality, a structure will have a different input impedance at each location, similar signals into the shakers will produce different forces. The best way to avoid any potential problems, however, is to have a low coherence between forces. This can be achieved by using either of two forcing methods: independent random signals at each shaker or simultaneous sine sweeps with each shaker having a different phase shift.

Another type of excitation is a free-decay response. A minor reformulation of the equations is involved, with Eq. (11) being modified to the form

$$-\left[[\ddot{X}_{i_{\mathrm{Re}}}][\ddot{X}_{i_{\mathrm{Im}}}]\right] = \left[[\tilde{C}_i][\tilde{K}_i]\right]\begin{bmatrix}[\dot{X}_{i_{\mathrm{Re}}}] & [\dot{X}_{i_{\mathrm{Im}}}]\\ [X_{i_{\mathrm{Re}}}] & [X_{i_{\mathrm{Im}}}]\end{bmatrix} \tag{19}$$

This formulation eliminates the need for measurement of the forces, thus allowing free-decay responses to be employed. This can also be used in conjunction with the Randomdec method, where a free-decay response is generated from a structure that is being randomly excited.

Averaging

There are two possible methods to eliminate noise contamination in the eigenvalue results. Both methods involve a type of signal averaging. The first method involves averaging spectra from several runs to form a single acceleration spectrum and force spectrum at each location before insertion into Eq. (13).

There is one serious drawback to this method. With random excitations, excessive averaging can produce a spectrum with a uniform value, effectively giving fewer independent columns in Eq. (13) with which to do a least-squares fit. For a swept-sine test, this averaging technique should suffice, since the spectra will not tend to become uniform, especially if the signal generator has a phase modulator.

The second method is to string the multiple runs together in the same manner as the individual frequencies were in Eq. (8). That is,

$$[\ddot{X}(w)] = \left[[\ddot{X}_1(w)]\,|\,[\ddot{X}_2(w)]\,|\ldots|\,[\ddot{X}_p(w)]\right]$$

This increases the number of columns, therefore, the accuracy of the least-squares fit, but the required storage space for the matrices is also increased.

Pseudo-Degrees of Freedom

If the structure being tested has more modes in the frequency range of interest than there are measurement locations, there is a technique to increase the number of DOFs based on existing measurement DOFs. This method involves sampling extra sets of data and placing each new set into the equations as if it represented new DOFs. With this approach is an alternate method in which the responses of the originally measured data are partitioned into subsets and correspondingly labeled as different sets of data. In this way the number of DOFs is increased without the need for more measurements. This, however, gives fewer columns of data for the least-squares process, since this procedure takes some of the columns in Eq. (8) and makes new rows out of them.

Mode Selection

Proper selection of the true modes of vibration from the eigensolution of Eq. (16) is just as important as any other part of the modal analysis. When the number of modes is overspecified, either through oversight or to compensate for noise contamination, a systematic method is needed to identify the spurious modes. Usually the spurious modes can be eliminated immediately by a quick examination of the eigenvalues. The damping values are often excessively high, low, or even negative. The natural frequencies might have values that are out of the measured frequency range. At other times, however, the spurious mode eigenvalues are within the range of tolerance. Then, an inspection of the eigenvectors is needed. One procedure involves the use of pseudo-DOFs. A comparison of the portion of the eigenvector representing the pseudo-DOFs with the portion of the eigenvector that corresponds to the independent DOFs from which the pseudo

DOFs were produced can readily determine the validity of the mode. A favorable relationship would be one where there is a high correlation of eigenvector values at corresponding DOFs. Another method would be to analyze results of analyses from several data sets; modes that repeatedly show up would indicate valid modes.

Simulation Studies

To verify the validity and accuracy of the MSMA technique previously described, several computer simulations were conducted. The primary concerns evaluated in the tests were: 1) resolution of the modes in high noise, 2) identification of modes less than $\xi_r w_r$ apart, 3) accuracy of modes at dependent DOFs, and 4) application of forces at dependent DOFs.

A computer program was designed such that the system natural frequencies, damping, and mode shapes, and a noise-to-signal ratio are input. The noise level is calibrated by using the rms of the response signal over the entire frequency range. Also input are the frequency range, number of independent DOFs and their corresponding locations, number of dependent DOFs and their locations, number of forced DOFs and their locations, and the method of excitation. The program creates the frequency responses for the accelerations and forces and then proceeds to manipulate them in accordance with the equations presented earlier.

The first series of tests was on system A having nine natural frequencies, seven of which were below 10 Hz. This series was conducted to evaluate the ability of the MSMA algorithm to resolve modes from noisy data and its ability to identify closely coupled modes. As noted in Table 1, two of the frequencies were selected less than $\xi_r w_r$ apart so that the effects of closely coupled modes could be observed. The noise-to-signal ratio was selected at 20% in conjunction with an applied random force signal. Changed during the test series was the number of forced DOFs: one, four, and eight forces were used. As indicated in Table 2a, the mode shapes had magnitudes of 1.0 at each station, except for one DOF in each mode whose magnitude was set at 0.01 to simulate a point close to a node line.

A sampling run was first made using a single shaker to obtain an estimate of the number of modes in the 0-10 Hz range. A check of the FRFs showed that six modes were fairly apparent; therefore, an estimate of eight modes (six for the observed ones and two more for any missed modes or any pseudo or spurious modes created by the noise) did not seem unreasonable.

Three runs were made for each of the force configurations plus one additional run utilizing the averaging technique of placing several runs into one large array. The averaged

Table 1 Natural frequencies and damping factors for simulated parameter identification tests

	System A		System B	
Mode	Frequency, Hz	Damping	Frequency, Hz	Damping
1	5.00	0.01	5.00	0.01
2	5.25	0.01	5.25	0.01
3	5.50	0.01	5.50	0.01
4	5.55	0.01	5.55	0.01
5	5.90	0.01	15.00	0.01
6	6.20	0.01	25.00	0.01
7	6.60	0.01		
8	15.00	0.01		
9	25.00	0.01		

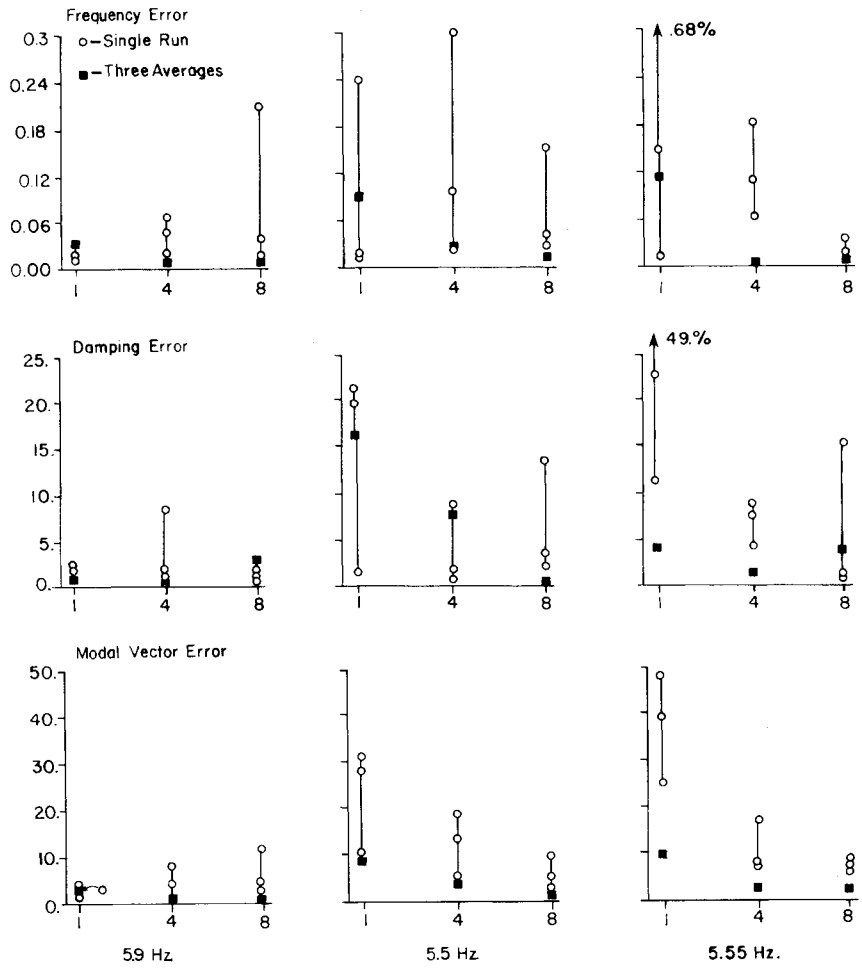

Fig. 1 Error comparisons for test series 1 (system A) noise/signal = 0.2, random noise excitation.

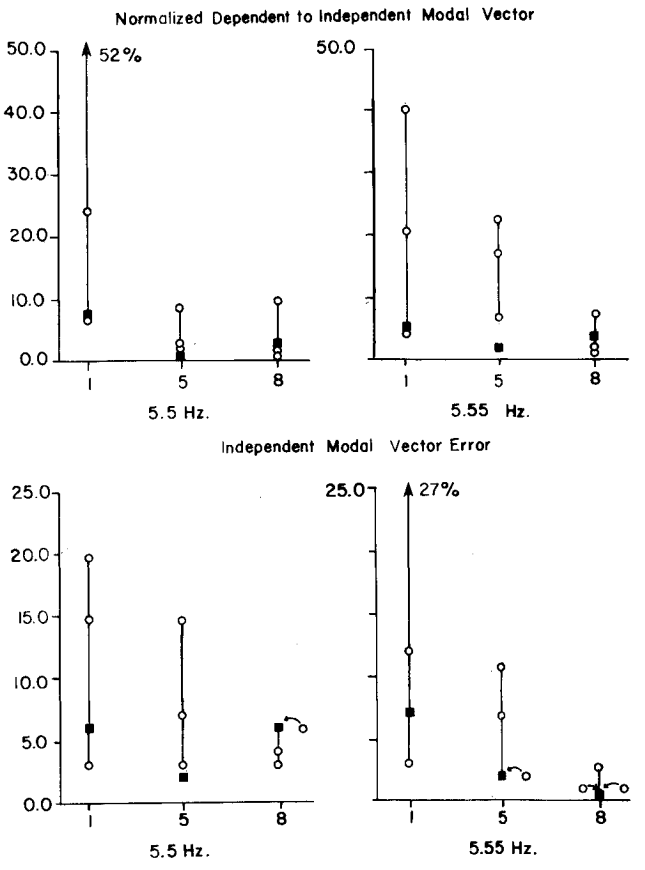

Fig. 2 Error comparisons for test series 2 (system B) noise/signal = 0.2, random noise.

analysis used three individual runs which differed from the previous three runs.

To check the accuracy of the results, an error analysis was used that looked at the percentage of error in the natural frequency, damping, and real part of the modal vector compared to the input system characteristics. To highlight the results, the errors for three modes were investigated. The first was the 5.9 Hz mode, which was relatively uncoupled. The other two modes were the coupled modes, 5.5 and 5.55 Hz. Referring to the diagrams in Fig. 1, it can be seen that with 20% noise the natural frequency estimates are highly accurate, even for the closely coupled modes. Also evident in the diagrams is the overall higher accuracy of the parameters corresponding to the 5.9 Hz mode compared to the 5.5 and 5.55 Hz modes. Although the errors for the damping and modal vectors are large for the 20% noise single-shaker case, the diagrams show a trend toward lower error levels as the number of shakers is increased. In fact, when eight shakers were employed, the error levels for the closely coupled modes are seen to be comparable to the error level for the 5.9 Hz mode.

System A was also employed in a series of tests on the effect of noise level. The noise-to-signal ratio was changed from 0 to 10% and finally to 20%. To illustrate the effect of noise on the results and the effect of additional shakers, the identified modal parameters for the 5.0, 5.5, and 5.55 Hz modes are tabulated for the single- and eight-shaker simulations (see Tables 3 and 4). An analysis of the tables shows, once again, a clear trend toward higher levels of accuracy at a given noise level for an increase in the number of shakers. A dramatic result from this set of runs was the absence of the 5.0 Hz mode from the single-shaker analysis when noise was present. As the number of shakers increased though, the 5.0 Hz mode appeared and then increased in accuracy. Overall, by a comparison of the tables, it is seen that the algorithm does not become unstable with increasing noise levels. On the contrary,

Table 2a System A mode shapes (defined at eight DOFs only); forces and locations

	Degrees of freedom							
Mode	1	2	3	4	5	6	7	8
1	0.01	1.00	1.00	1.00	1.00	1.00	1.00	1.00
2	1.00	0.01	1.00	1.00	−1.00	−1.00	−1.00	−1.00
3	1.00	1.00	−0.01	−1.00	−1.00	−1.00	1.00	1.00
4	1.00	1.00	−1.00	−0.01	1.00	1.00	−1.00	−1.00
5	1.00	−1.00	−1.00	1.00	0.01	−1.00	−1.00	1.00
6	1.00	−1.00	−1.00	1.00	−1.00	0.01	1.00	−1.00
7	1.00	−1.00	1.00	−1.00	−1.00	1.00	−0.01	1.00
8	1.00	−1.00	1.00	−1.00	1.00	−1.00	1.00	−0.01
9	1.00	1.00	1.00	1.00	1.00	1.00	1.00	1.00

No. of forces	Force locations
1	1
4	1-4
8	1-8

Table 2b System B mode shapes (defined at eight DOFs only); forces and locations

	Degrees of freedom							
Mode	1	2	3	4	5	6	7	8
1	0.01	1.00	1.00	1.00	1.00	1.00	1.00	1.00
2	1.00	0.01	1.00	1.00	−1.00	−1.00	−1.00	−1.00
3	1.00	1.00	−0.01	−1.00	−1.00	−1.00	1.00	1.00
4	1.00	1.00	−1.00	−0.01	1.00	1.00	−1.00	−1.00
5	1.00	−1.00	−1.00	1.00	0.01	−1.00	−1.00	1.00
6	1.00	−1.00	−1.00	1.00	−1.00	0.01	1.00	−1.00

No. of forces	Force locations
1	1
5	1-5
8	1-8

Table 3a Identified modal parameters for system A (No. of forces = 1, noise ratio = 0.0)

Undamped natural frequency	5.0063	5.5000	5.5498
Damping factor	0.0143	0.0100	0.0100
DOF		Modal coefficient	
Re(1)	0.00308	0.99605	−0.99496
Re(2)	0.99493	0.99698	−0.99296
Re(3)	0.99824	−0.00735	0.99870
Re(4)	0.99609	−0.99690	0.95447
Re(5)	0.99875	−0.99868	−0.99729
Re(6)	0.99814	−0.99871	−0.99735
Re(7)	1.00000	1.00000	1.00000
Re(8)	0.99931	0.99989	0.99973
Im_{max}	0.02780	0.00769	0.00062

Table 3b Identified modal parameters for system A (No. of forces = 1, noise ratio = 0.1)

Undamped natural frequency	No 5 Hz mode identified	5.4982	5.5657
Damping factor		0.0092	0.0126
DOF		Modal coefficient	
Re(1)		1.00000	0.96980
Re(2)		0.96169	1.00000
Re(3)		−0.11159	−0.60195
Re(4)		−0.95309	−0.03063
Re(5)		−0.86633	0.66319
Re(6)		−0.87422	0.65522
Re(7)		0.85209	−0.57500
Re(8)		0.85267	−0.64153
Im_{max}		0.24759	0.29919

Table 3c Identified modal parameters for system A (No. of forces = 1, noise ratio = 0.2)

Undamped natural frequency	No 5 Hz mode identified	5.5003	5.5879
Damping factor		0.0098	0.0110
DOF		Modal coefficient	
Re(1)		0.89703	−0.72131
Re(2)		1.00000	−0.56014
Re(3)		−0.26396	0.83339
Re(4)		−0.71778	−0.07690
Re(5)		−0.09235	−0.41497
Re(6)		−0.17339	−0.50867
Re(7)		0.55184	1.00000
Re(8)		0.51095	0.94717
Im_{max}		0.21516	0.06490

Table 4a Identified modal parameters for system A (No. of forces = 8, noise ratio = 0.0)

Undamped natural frequency	4.9966	5.5000	5.5499
Damping factor	0.0099	0.0100	0.0100
DOF		Modal coefficient	
Re(1)	0.01429	1.00000	−0.99759
Re(2)	1.00000	0.99934	−0.99663
Re(3)	0.99818	−0.01186	0.99938
Re(4)	0.99943	−0.99939	0.00978
Re(5)	0.99744	−0.99812	−0.99870
Re(6)	0.99777	−0.99810	−0.99873
Re(7)	0.99667	0.99719	1.00000
Re(8)	0.99707	0.99726	0.99987
Im_{max}	0.00086	0.00228	0.00064

Table 4b Identified modal parameters for system A (No. of forces = 8, noise ratio = 0.1)

Undamped natural frequency	4.9980	5.5058	5.5490
Damping factor	0.0097	0.0103	0.0100
DOF		Modal coefficient	
Re(1)	0.02516	−0.98585	0.98362
Re(2)	0.98621	−0.99463	1.00000
Re(3)	1.00000	0.02763	−0.95197
Re(4)	0.98411	1.00000	−0.06453
Re(5)	0.97350	0.94609	0.87503
Re(6)	0.97147	0.95297	0.87421
Re(7)	0.97307	−0.98640	−0.88674
Re(8)	0.96948	−0.95976	−0.89013
Im_{max}	0.02016	0.06440	0.21813

Table 4c Identified modal parameters for system A (No. of forces = 8, noise ratio = 0.2)

Undamped natural frequency	5.0007	5.4918	5.5512
Damping factor	0.0093	0.0079	0.0100
DOF		Modal coefficient	
Re(1)	0.00020	1.00000	−0.83500
Re(2)	0.99549	0.97812	−0.82366
Re(3)	0.98808	−0.00563	0.92143
Re(4)	0.99560	−0.94902	−0.06190
Re(5)	0.99595	−0.92819	−0.96699
Re(6)	0.98004	−0.95929	−0.96398
Re(7)	0.98590	0.96932	1.00000
Re(8)	1.00000	0.98243	0.96990
Im_{max}	0.05798	0.18716	0.18870

good results are obtained even at relatively high noise levels when several shakers are used.

A second series of tests was performed to assess the accuracy with which the MSMA algorithm computes modal coefficients at dependent DOF's and to test its ability to employ forces at dependent DOF's. System B (see Table 1), an eight-DOF system with four modes in the 0-10 Hz range, was used. In this case the noise-to-signal ratio was also 20%, but the number of forces was set at 1, 5, and 8 (an initial sampling run indicated three, possibly four, modes present in the 0-10 Hz range, so five independent DOFs were selected).

The previous series of tests was again performed, but since the only substantial errors occurred in the coupled modes, their parameters were the only ones analyzed. In this analysis, only the normalized independent modal vectors and a ratio of the normalized dependent to independent modal vectors were calculated (see Fig. 2).

Again, a convergence toward higher accuracy is seen in these results as the number of applied forces is increased. An important feature of the results is that the accuracy of the dependent DOFs, calculated from Eq. (18), follows closely the same trends as the independent DOFs. Also to be noted in the diagrams are the error levels for five and eight shakers. Although three shakers are exciting dependent DOFs in the eight-shaker case, the accuracy is either maintained or improved in almost every instance. Even if there happens to be a higher error indication for an increase in shakers, there is a definite lessening in the error spread.

Two more series of tests were run. The first was a set of runs identical to the first test case with the exception that the forc-

ing functions were swept-sines instead of random excitation. The results of this set were basically identical to the random excitation set. The final series also used the same setup as the first test, except that no noise was introduced and the test range was from 0-1024 Hz with 256 data points (a delta frequency of over 4 Hz). The ninth mode corresponding to 25 Hz was also deleted. All modes were identified to extremely high accuracy (the error was less than 1 part per billion) in spite of the fact that there were seven natural frequencies between two of the data points!

Conclusions

The modal parameter estimation algorithm of Coppolino has been extended to permit multiple-exciter testing. Reduced system matrices are computed by a least-squares procedure using Fourier-transformed input forces and acceleration responses, and modal parameters are then calculated from these system matrices. The algorithm here bears some resemblance to the direct system parameter identification algorithm of Leuridan et al. The most significant differences between the present and the Leuridan algorithms are the order of the system matrices identified and the procedure employed for computing mode shapes. Although the present algorithm is developed for systems having "proportional damping," it can easily be extended to general linear time-invariant systems.

The validity of the proposed multi-shaker modal analysis (MSMA) method was demonstrated analytically through an extensive computer simulation study. The computer simulation showed the MSMA method to be stable in the presence of random noise, and demonstrated the potential of the method to identify closely spaced frequency modes.

Acknowledgments

This work was supported by NASA Contract NAS8-33980 with Marshall Space Flight Center. The interest and encouragement of the contract monitor, Larry Kiefling, are gratefully acknowledged.

References

[1]Lewis, R. C. and Wrisley, D. L., "A System for the Excitation of Pure Natural Modes of Complex Structures," *Journal of the Aeronautical Sciences*, Vol. 17, No. 11, 1950, pp. 705-722.

[2]Anderson, S. E., "Another Look at Sine-Dwell Mode Testing," *Proceedings of the AIAA/ASME/ASCE/AHS 22nd Structures, Structural Dynamics and Materials Conference*, Pt. 2, April 1981, pp. 202-211.

[3]Smith, W. R., "Least-Squares Time-Domain Method for Simultaneous Identification of Vibration Parameters from Multiple Free-Response Records," *Proceedings of the AIAA/ASME/ASCE/AHS 22nd Structures, Structural Dynamics and Materials Conference*, Pt. 2, April 1981, pp. 194-201.

[4]Ibrahim, S. R. and Mikulcik, E. C., "A Method for the Direct Identification of Vibration Parameters from Free Response," *Shock and Vibration Bulletin*, Bull. 47, Pt. 4, Sept. 1977, pp. 183-198.

[5]Pappa, R. S., "Close-Mode Identification Performance of the ITD Algorithm," *Proceedings of the AIAA/ASME/ASCE/AHS 24th Structures, Structural Dynamics and Materials Conference*, Pt. 2, May 1983, pp. 193-205.

[6]Richardson, M., "Modal Analysis Using Digital Test Systems," *Seminar on Understanding Digital Control and Analysis in Vibration Test Systems*, The Shock and Vibration Information Center, Washington, D.C., May 1975, pp. 43-64.

[7]Allemang, R. J., "Investigation of Some Multiple Input/Output Frequency Response Function Experimental Modal Analysis Techniques," Ph.D. Dissertation, University of Cincinnati, Ohio, 1980.

[8]Kennedy, C. C. and Pancu, C. D. P., "Use of Vectors in Vibration Measurement," *Journal of the Aeronautical Sciences*, Vol. 14, Nov. 1947, pp. 603-625.

[9]Craig, R. R. and Su, Y-W. T., "On Multiple Shaker Resonance Testing," *AIAA Journal*, Vol. 12, July 1974, pp. 924-931.

[10]Richardson, M. and Kniskern, S., "Identifying Modes of Large Structures from Multiple Input and Response Measurements," SAE Paper 760875, Nov. 1976.

[11]Brown, D. L., Allemang, R. J., Zimmerman, R., and Mergery, M., "Parameter Estimation Techniques for Modal Analysis," *SAE Transactions*, Vol. 88, Sec. 1, 1979, pp. 828-846.

[12]Ensminger, R. R. and Turner, M. J., "Structural Parameter Identification from Measured Vibration Data," *Proceedings of the AIAA/ASME/ASCE/AHS 20th Structures, Structural Dynamics and Materials Conference*, April 1979, pp. 410-416.

[13]Coppolino, R. N., "A Simultaneous Frequency Domain Technique for Estimation of Modal Parameters from Measured Data," SAE Paper 811046, Oct. 1981.

[14]Vold, H., Kundrat, J., Rocklin, G. E., and Russell, R., "A Multi-Input Modal Estimation Algorithm for Mini-Computers," SAE Paper 820194, 1982.

[15]Leuridan, J. M., Brown, D. L., and Allemang, R. J., "Direct System Parameter Identification of Mechanical Structures with Application of Modal Analysis," *Proceedings of the AIAA/ASME/ASCE/AHS 23rd Structures, Structural Dynamics and Materials Conference*, May 1982, pp. 548-556.

[16]Hendricks, S. L., Rajaram, S., Kamat, M. P., and Junkins, J. L., "Identification of Large Flexible Structures Mass/Stiffness and Damping from On-Orbit Experiments," *Journal of Guidance, Control, and Dynamics*, Vol. 7, March-April 1984, pp. 244-245.